Dean&Francis
ISSN 2959-6157

Design of a BUCK Converter Achieving TCM-ZVS via V^{2}C Control

Shunpeng Xu[1],

Ming Xie[2]

[1]University of Shanghai for Science and Technology,Shanghai,China,200093
[2]University of Shanghai for Science and Technology,Shanghai,China,200093
[1]email:seasible@outlook.com
[2]email:elecxm@usst.edu.cn

Abstract:

By analyzing the simplified MOSFET equivalent output capacitance (C_{oss}) model, the minimum reverse current required for soft switching and the corresponding dead time in a synchronous BUCK converter operating in Triangular Current Mode (TCM) are calculated. A readily implementable peak-current control strategy is adopted to achieve zero-voltage switching (ZVS) under TCM. Furthermore, a V2C control method is employed to introduce appropriate slope compensation to the control voltage, effectively eliminating subharmonic oscillations when the duty cycle $D>0.5$. The calculated values are verified through simulations in MATLAB/Simulink. Ultimately, a synchronous BUCK converter with a wide output voltage range is designed, which achieves ZVS across the entire operating range in TCM, minimizes inductor current ripple, and features a simple control scheme.

Keywords: BUCK converter, Triangular Current Mode (TCM), V^{2}C Control, zero-voltage switching (ZVS)

1. Introduction

The synchronous BUCK converter, whose circuit structure is shown in Figure1, integrates synchronous rectification technology into the traditional BUCK topology. It offers advantages such as high efficiency, compact size, and a simple topology. However, as the operating frequency increases, switching losses within the converter become significantly more pronounced [1].

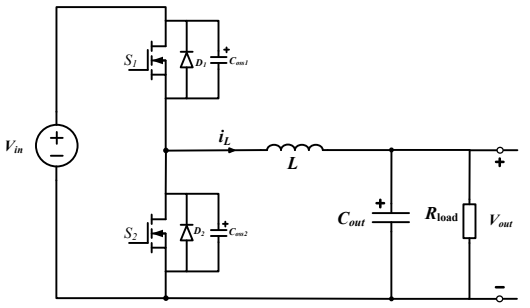

Figure 1 synchronous BUCK converter

Soft-switching techniques enable the realization of

ISSN 2959-6157

high-efficiency, high-frequency switching converters. The Triangular Current Mode (TCM) leverages the reverse zero-crossing of inductor current to achieve soft switching. This approach induces resonance between the inductor and the parasitic capacitances of the MOSFETs through the reverse current generated by the inductor current zero-crossing, thereby realizing ZVS [2].

Previous studies [3, 4] have implemented TCM control via variable-frequency modulation. However, this method relies heavily on the accuracy of mathematical models and demands high-performance controllers, leading to increased overall converter costs.

To ensure control precision and stability while simplifying the control strategy, the wide-output-range BUCK converter presented in this paper adopts a peak-current control strategy to achieve TCM operation.

Research on peak-current control in switching converters has demonstrated that subharmonic oscillations occur when the duty cycle D>0.5 .[5] Therefore, a control strategy must be implemented to mitigate this phenomenon. To achieve precise control of the inductor current peak and stabilize the output voltage at the target value for TCM-ZVS, the control system fundamentally employs a voltage loop as the outer loop and an inductor current loop as the inner loop. However, this approach does not significantly improve the transient response to sudden load changes.

Compared to conventional current-mode or voltage-mode control techniques, V^2 control offers faster transient response [6, 7]. Yet, its stability deteriorates when the equivalent series resistance (ESR) of the filter capacitor is small [8]. The V2C control method combines the advantages of current-mode control and V^2 control. This approach is straightforward for engineering applications, enhances both dynamic and steady-state performance [9, 10], and simultaneously eliminates harmonic oscillation issues.

This paper achieves a BUCK converter capable of full TCM - ZVS across a wide output range through V2C control. Its functionality is validated through simulations in MATLAB/Simulink.

2. Implementation Principle of TCM-ZVS

The fundamental concept of achieving zero-voltage switching (ZVS) in Triangular Current Mode (TCM) involves reversing the inductor current for a specific duration to discharge the output capacitance of the switch before its turn-on. However, excessive reverse time leads to increased reverse current, elevated inductor current ripple, and intensified losses in the inductor. Therefore, precise control of the reverse current magnitude is critically important.

2.1 MOSFET Parasitic Output Capacitance (C_{oss}) Model

To accurately determine the reverse current value, a mathematical model of the MOSFET's Coss must first be established. A triangular model is employed to characterize Coss, as this approach has been validated to most closely approximate the actual drain-source voltage and inductor current waveforms, enabling precise estimation of the minimum required current [11]. The corresponding mathematical formulation is given by:

$$V_c = \begin{cases} V_{out}, & q_c > Q_c \\ 0, & q_c \leqslant Q_c \end{cases}$$

2.2 Analysis of TCM Mode [12]

Figure 2 shows the key waveform diagrams of the BUCK converter in TCM mode.

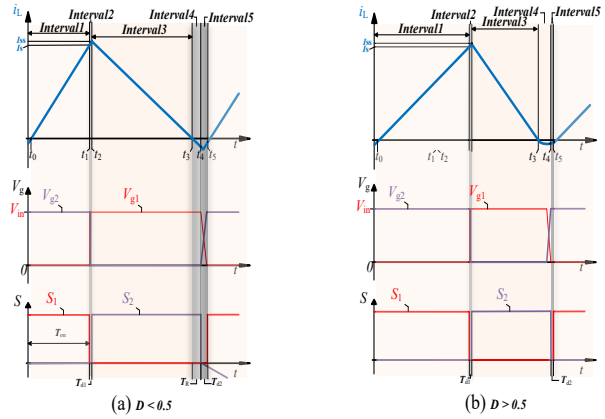

Figure 2 Key Waveform Diagrams

Interval 1 ($t_0 \sim t_1$): S_1 is turned off and S_2 is turned on. The input voltage V_{in} charges the inductor L, and at t_1, the inductor current reaches I_s. It can be obtained that the rising slope m_1 of the inductor current is:

$$m_1 = \frac{V_{in} - V_{out}}{L}$$

Interval 2 ($t_1 \sim t_2$): S_1 is turned off and S_2 is turned off. This interval is the dead – time T_{d1}. During this interval, C_{oss1} is charged and C_{oss2} is discharged, and resonance will occur. However, since the resonance time is very short, the peak current I_{ss} after resonance is regarded as I_s. Until the voltage of C_{oss1} is V_{in} and the voltage of C_{oss2} is 0, the resonance ends. At this time, the conditions for soft - switching are met.

Interval 3 ($t_2 \sim t_3$): S1 is turned off and S2 is turned on. S2 is turned on softly, and the inductor current continues to decline until it reaches 0. The declining slope m_2 is:

$m_2 = \frac{V_{out}}{L}$ Interval 4 ($t_3 \sim t_4$): There are two cases in this stage: 1. The duty cycle D<0.5 ; 2. The duty cycle D>0.5 .

For the first case, S1 is turned off and S2 is turned on. A reverse current is required, and the conduction time of S2 needs to be deliberately extended until I_R . The reverse current part is enlarged as shown in Figure 3. This case is the critical situation for achieving TCM - ZVS. At this time, through geometric analysis, the calculation formulas for I_R and T_R can be obtained:

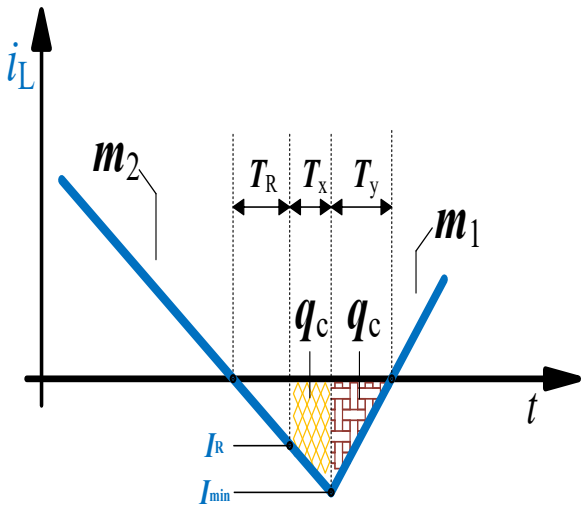

Figure 3 the reverse current

$$I_R = \sqrt{\frac{2q_c(V_{in} - 2V_{out})}{L}}$$

$$T_R = \frac{\sqrt{2q_c(V_{in} - 2V_{out})L}}{V_{out}}$$

For the second case, no reverse current is required. S1 is turned off and S2 is turned off. Coss1 starts to discharge to 0, and Coss2 starts to charge to V_{in} . At this time, the conditions for ZVS are met as shown in Figure 2 (b)

Interval 5 ($t_4 \sim t_5$): For the first case, S1 is turned off and S2 is turned off. At this time, the dead-time T_{d2} needs to be deliberately extended to meet the ZVS conditions. Through geometric analysis, we can get:

$$\begin{cases} I_{\min} = \dfrac{\sqrt{2q_c(V_{in} - V_{out})L}}{V_{out}} \\ T_x = \dfrac{I_{min} - I_R}{m_2} \\ T_y = \dfrac{2q_c}{I_{\min}} \\ T_{d2} = T_x + T_y \end{cases}$$

For the second case, soft - switching can be achieved regardless of when it is turned on.

3. Simulation Analysis and Issues of TCM Mode

Based on the above formulas, the peak value of the inductor current can be calculated. The formula is as follows: Consequently, a peak - comparison method is employed to control the inductor current. After calculating Is, T_{d1} , and T_{d2} according to the previous formulas, a model of this BUCK converter is built in MATLAB/Simulink.

The following results are obtained:

Operating condition: Input voltage is 48 V, output voltage is 12 V, and duty cycle D=0.25 as shown in Figure 4(a)

Operating Condition: Input Voltage is 48 V, Output Voltage is 30 V, and Duty Cycle D=0.625 as shown in Figure 4(b)

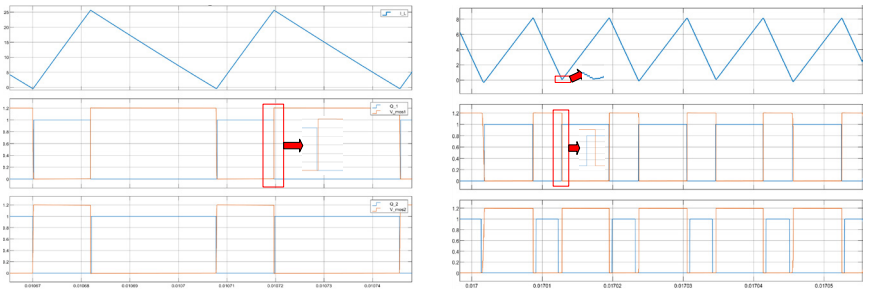

(a) ***D < 0.5*** (b) ***D > 0.5***

Figure 4. the waveform diagrams of simulation

ISSN 2959-6157

As can be observed from the waveform diagrams, when the duty cycle D>0.5 , the inductor current fails to stably cross zero, resulting in the inability to fully achieve soft - switching.

3. V²C Control Method

To address this issue, this paper introduces the V²C control method. In this control strategy, the outer loop compares the detected output voltage with the reference voltage V_{ref} . The resulting error is processed by an error amplifier to generate the control voltage v_c . The inner loop utilizes a feedback quantity derived from the weighted combination of the inductor current and the output voltage, where ω_c and ω_V are the weighting factors for the inductor current and the output voltage, respectively. The feedback inner loop of V²C control is equivalent to introducing output voltage feedback into the current feedback loop of peak-current control. The system block diagram is shown in Figure 5.

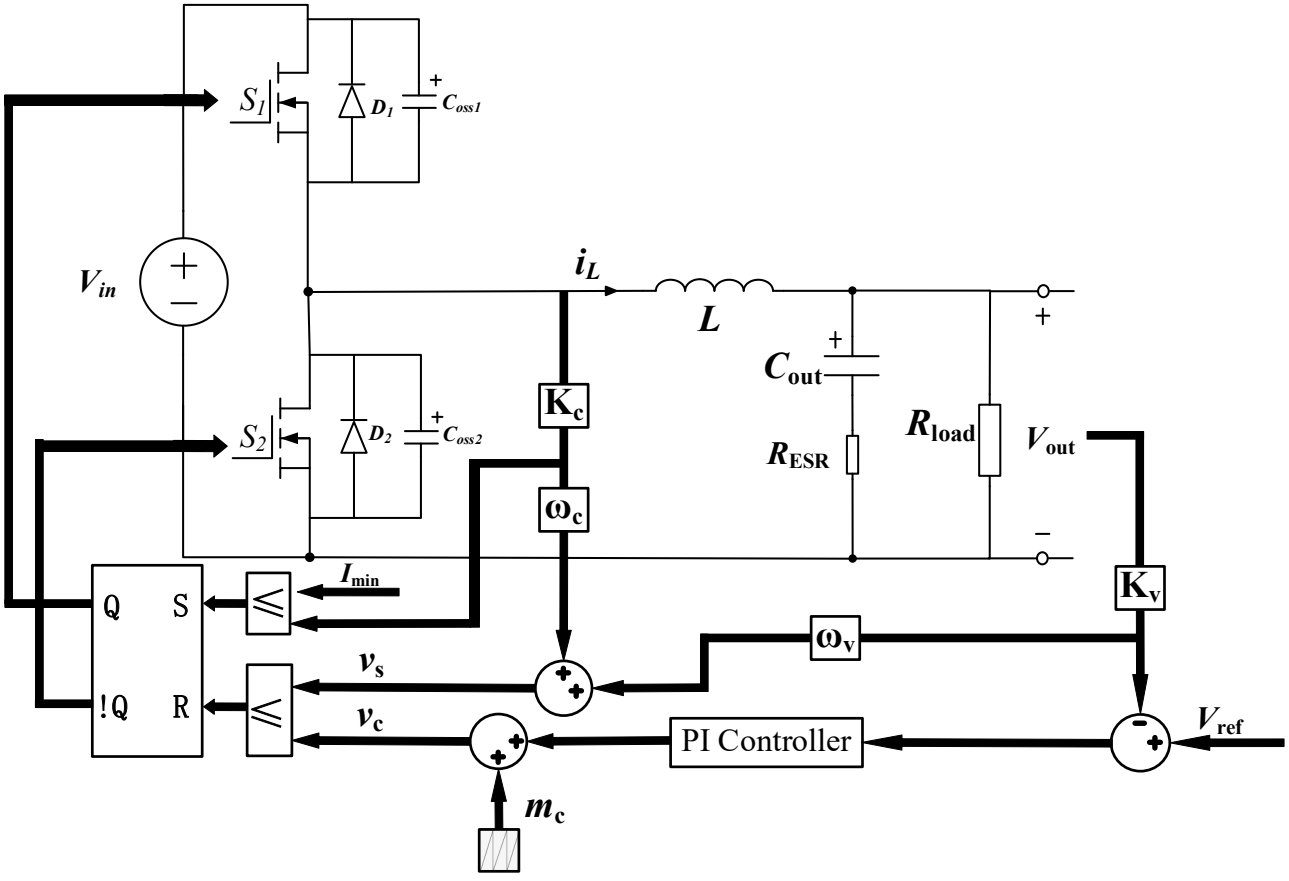

Figure 5. V²C control mode BUCK converter

The compensation slope m_c and the compensator need to be determined through small-signal modeling.

3.1 Small - Signal Model Analysis

The inductor current waveforms with and without slope compensation are shown in Figure 6.

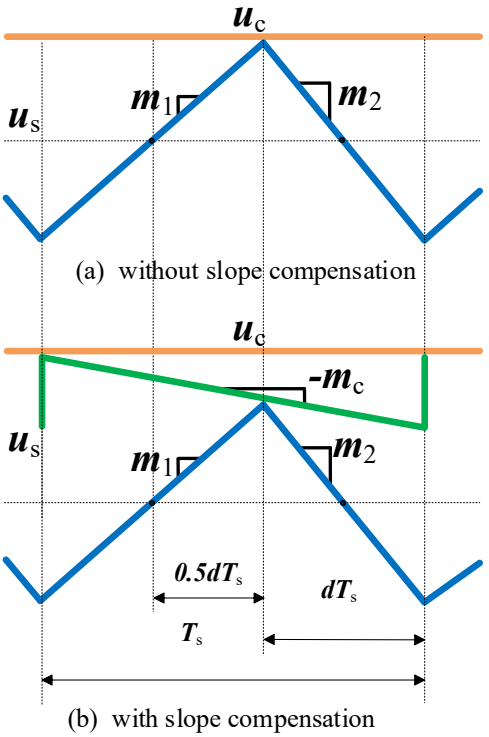

Figure 6. inductor current waveforms with and without slope compensation

The expressions for these two cases can be derived through calculation as follows:

$$\frac{m_1 dT_s}{2} = \begin{cases} v_c - v_s \\ v_c - v_s - m_c dT_s \end{cases}$$ where:

$v_s = \omega_c K_c i_L + \omega_V K_V v_{out}$ By applying small-signal perturbations to the variables in the equation and neglecting second-order small-signal terms, the following expressions can be obtained:

$$\hat{d} = F_c \hat{v}_c - F_v \hat{v}_{out} - F_i \hat{i}_L - F_{in} \hat{v}_{in}$$

where:

Without slope compensation:

$$\begin{cases} F_c = \dfrac{2}{m_1 T_s} \\ F_v = \dfrac{2\omega_v K_v}{m_1 T_s} - \dfrac{D^2}{(1-D)V_{out}} \\ F_i = \dfrac{2\omega_c K_c}{m_1 T_s} \\ F_{in} = \dfrac{D^2}{(1-D)V_{out}} \end{cases}$$

With slope compensation:

By applying the established method for constructing the small-signal model of the converter power stage, the small-signal model relating the control voltage to the output voltage can be derived as follows:

$\hat{v}_{out}$

Figure 6. Control System Block Diagram

where the expressions for the open-loop transfer functions $G_{vd}(s)$ and $G_{id}(s)$ are as follows:

$$G_{vd}(s) = \frac{V_{in}}{D} \frac{1}{f(s)}$$

$$G_{id}(s) = \frac{V_{in}}{DR_{load}} \frac{(1+sR_{load}C)}{f(s)}$$

where:

The transfer function from the output voltage v_{out} to the error signal uc is derived as follows:

Literature [13] analytically determines the minimum value of the compensation slope:

$$m_c > \frac{m_2 - m_1}{2}$$

4. Circuit Simulation Analysis

4.1 TCM - ZVS Realization under D > 0.5

After incorporating the V^2C control, as shown in Figure 8, it can be observed that the inductor current ripple remains stable, and zero - crossing is always guaranteed, thus achieving TCM - ZVS.

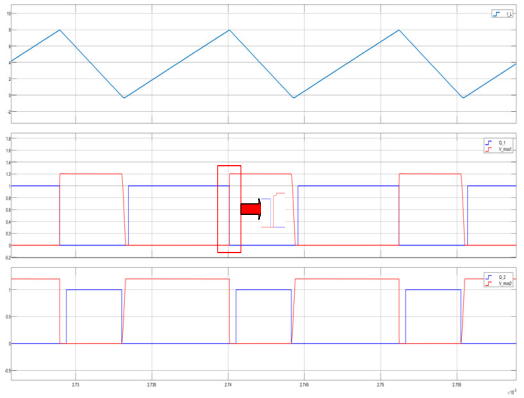

Figure 7. the waveform of V^2C control

ISSN 2959-6157

4.2 Comparison of Transient Response Characteristics of the Converter

The load-step response and target-voltage-step response of the inductor-current control and the V^2C control are compared.[14] The simulation results are shown in Fig. 8 and Fig. 9, respectively.

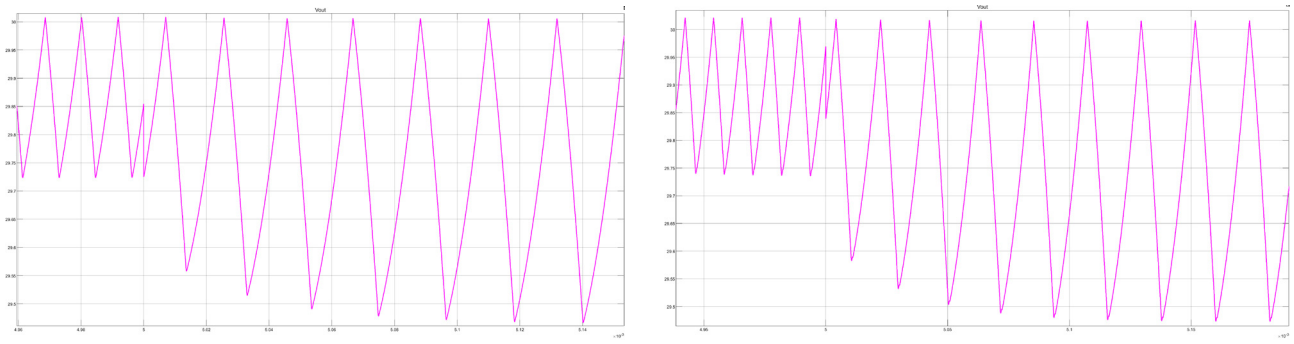

(a) V^2C control (b) I_L control

Figure 8. the waveform of load-step response

Results are compared in Table 1.

Table 1. the Settling Time of load-step response

Control Method	Load-step response
	Settling Time
V^2C Control	74.98us
Inductor Current Control	100.50us

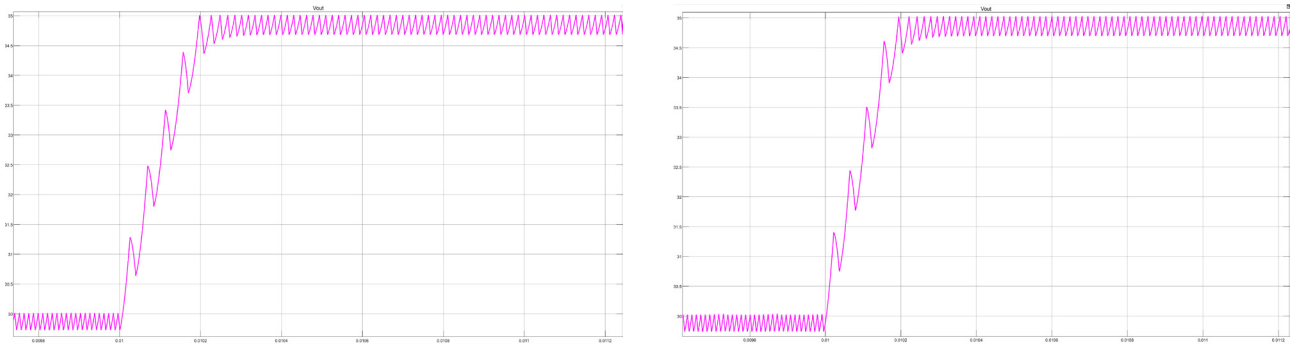

(a) V^2C control (b) I_L control

Figure 9. the waveform of target-voltage-step response

Results are compared in Table 2.

Table 2. the Settling Time of target-voltage-step response

Control Method	Target-voltage-step response (15V-30V)
	Settling Time
V^2C Control	489.67us
Inductor Current Control	637.09us

The simulation results show that, in terms of control effectiveness, compared with the traditional inductor - cur-

rent control, the V^2C control has better dynamic response performance, whether under load disturbances or during output target value switching. Therefore, when achieving the high - efficiency and wide - range TCM - ZVS mode through the peak - control method, V^2C is a good control strategy.

5. Conclusion

This paper proposes and analyzes a wide-output-range synchronous BUCK converter employing a V^2C control scheme, which achieves full-range zero-voltage switching in Triangular Current Mode.

By effectively integrating TCM-ZVS operation based on peak-current control with the V^2C control method, the inherent limitations of each individual technology are addressed. First, a simplified triangular model of Coss is adopted to derive key analytical expressions for the minimum reverse current ($I_{\min}$) required to achieve ZVS and its associated dead time (T_{d2}). Second, the proposed V^2C control strategy introduces a compensated voltage ramp, which not only eliminates subharmonic oscillations—issues that plague traditional peak-current-mode control when the duty cycle exceeds 0.5—but also significantly enhances transient response performance compared to the standard voltage-loop-plus-PI-current-loop control. The minimum compensation slope required for stability and the corresponding compensator are designed by establishing the system's small-signal model, with both frequency-domain simulations and final circuit simulations verifying the stability of the design.

MATLAB/Simulink simulation results under various operating conditions validate the effectiveness of the proposed method. The converter maintains stable TCM operation with inductor current zero-crossing, thereby achieving ZVS across the specified output voltage range. Compared to variable-frequency control, peak-current control demonstrates greater convenience in both theoretical derivation and practical design. Furthermore, comparative analysis further confirms the superiority of the V^2C control in dynamic response relative to traditional current-mode control.

References

[1] Xunwei Zhou, T. G. Wang and F. C. Lee, "Optimizing design for low voltage DC-DC converters," *Proceedings of APEC 97 - Applied Power Electronics Conference*, Atlanta, GA, USA, 1997, pp. 612-616 vol.2, doi: 10.1109/APEC.1997.575633.

[2] D. Christen, S. Tschannen and J. Biela, "Highly efficient and compact DC-DC converter for ultra-fast charging of electric vehicles," *2012 15th International Power Electronics and Motion Control Conference (EPE/PEMC)*, Novi Sad, Serbia, 2012, pp. LS5d.3-1-LS5d.3-8, doi: 10.1109/EPEPEMC.2012.6397481.

[3] Baocheng Wang, Ye Yuan, Yang Zhou and Xiaofeng Sun, "Buck/boost bidirectional converter TCM control without zero-crossing detection," *2016 IEEE 8th International Power Electronics and Motion Control Conference (IPEMC-ECCE Asia)*, Hefei, 2016, pp. 3073-3078, doi: 10.1109/IPEMC.2016.7512786.

[4] G. Yu, S. Yadav, J. Dong and P. Bauer, "Revisiting the Reverse Switched Current of Buck, Boost, and Buck–Boost Converters in Voltage-Mode TCM–ZVS Control Considering Parasitic Resistances," in *IEEE Transactions on Power Electronics*, vol. 39, no. 7, pp. 8254-8268, July 2024, doi: 10.1109/TPEL.2024.3382051.

[5] Mammano R. Switching power supply topology voltage mode vs. current mode[J]. Elektron Journal-South African Institute of Electrical Engineers, 2001, 18(6): 25-27.

[6] Fengyan Wang, Songrong Wu, Jianping Xu and Junfeng Xu, "Modeling and simulation of V/sup 2/ controlled switching converters," *The Fifth International Conference on Power Electronics and Drive Systems, 2003. PEDS 2003.*, Singapore, 2003, pp. 613-617 Vol.1, doi: 10.1109/PEDS.2003.1282923.

[7] Cortés J, Jiménezy J C, Jayasuriyay S, et al. Design-oriented stability criteria of av 2 control compensated with inductor current of a boost converter for shipboard power systems[C]//2015 IEEE Applied Power Electronics Conference and Exposition (APEC). IEEE, 2015: 2892-2897.

[8] J. Cortés, V. Šviković, P. Alou, J. A. Oliver, J. A. Cobos and R. Wisniewski, "Accurate Analysis of Subharmonic Oscillations of V2 and V2Ic Controls Applied to Buck Converter," in *IEEE Transactions on Power Electronics*, vol. 30, no. 2, pp. 1005-1018, Feb. 2015, doi: 10.1109/TPEL.2014.2308015.

[9] H. Li, Y. Liu, L. Zhao and Z. Li, "The communication power system with V2C adaptive control method," *2015 IEEE International Telecommunications Energy Conference (INTELEC)*, Osaka, Japan, 2015, pp. 1-6, doi: 10.1109/INTLEC.2015.7572338.

[10] Wang F, Xu J, Wang B. Comparison study of switching DC-DC converter control techniques[C]//2006 international conference on communications, circuits and systems. IEEE, 2006, 4: 2713-2717.

[11] Marxgut C B. Ultra-flat isolated single-phase AC-DC converter systems[D]. ETH Zurich, 2013.

[12] Youm J H, Do H L, Kwon B H. A single-stage electronic ballast with high power factor[J]. IEEE Transactions on Industrial Electronics, 2000, 47(3): 716-718.

[13] Zhou G, Xu J, Mi C, et al. Stability analysis of V (2) C controlled buck converter[J]. Diangong Jishu Xuebao(Transactions of China Electrotechnical Society), 2011, 26(3): 88-95.

[14] Narasimharaju B L. Enhanced closed loop voltage control of buck converter for improved performance[C]//2014 Annual IEEE India Conference (INDICON). IEEE, 2014: 1-5.